Automatic Detection Method of Mining subsidence basin based on InSAR and CNN-AFSA-SVM

Lei Wang (austwlei@163.com)
Anhui University of Science and Technology https://orcid.org/0000-0001-8483-0471
Shibao Li
Anhui University of Science and Technology
Chuang Jiang
Anhui University of Science and Technology
Chaoqun Teng
Anhui University of Science and Technology
Jingyu Li
Anhui University of Science and Technology
Zhong Li
Anhui University of Science and Technology
Jinzhong Huang
Anhui University of Science and Technology

Research Article

Keywords: mining subsidence, differential radar interferometry, convolutional neural network, support vector machine

Posted Date: February 7th, 2022

DOI: https://doi.org/10.21203/rs.3.rs-1250242/v1

Abstract

Mining subsidence disasters are common geological disasters. Accurate and effective identification of their deformation position is significant in preventing and controlling geological disasters and monitoring illegal mining. In this study, we used deep learning combined with support vector machine (SVM) to establish an automatic detection method for mining subsidence basins using Sentinel-1A data. The Huainan mining area was selected as the experimental area to verify the method. The interferogram was obtained using differential radar interferometry (D-InSAR), and the mining subsidence basin and other targets were extracted manually as training samples. Subsequently, AlexNet, VGG19, and ResNet50 convolutional neural networks (CNNs) were used to extract feature vectors of mining subsidence basins for the SVM classifier, and mining subsidence basins were detected in a large-area InSAR interferogram; The artificial fish swarm algorithm with strong optimization ability and good global convergence is introduced into SVM parameter optimization to construct an improved ResNet50_ SVM model. The experimental results show that (1) the three CNN_SVM methods can accurately detect dry mining subsidence basins automatically in large regional interference maps, providing an essential scientific basis for the government to monitor illegal mining activities and prevent and control geological disasters in mining areas; (2) the accuracy of the CNN_SVM automatic detection methods for mining subsidence basins is approximately 80%, and that of ResNet50_SVM for mining subsidence basin detection is 83.7%, superior to that of AlexNet_SVM and VGG19_SVM, The accuracy of the improved ResNet50_SVM based on AFSA algorithm is 88.3%, which is better than the unimproved Resnet50_SVM model.

Introdution

The original stress equilibrium state of overlying strata may be easily broken by mining mineral resources, resulting in strata and surface movement and deformation. This causes a series of geological and environmental disasters in mines, threatening the safety of life and property of mining residents(Zhu et al. 2017). Therefore, to conduct efficient and accurate monitoring of mining activities in mining areas, it is crucial to prevent geological and environmental disasters caused by mining. Moreover, these measures can provide a scientific basis for government departments to supervise illegal mining activities.

Currently, the government mainly monitors illegal mining activities according to the traditional investigation method of "carpet type," and some use microseismic and information network. These methods are inefficient and have a small scope for monitoring large-scale illegal mining activities. Despite certain prevention and control measures, illegal mining has been repeatedly banned. According to the State Administration of Work Safety statistics, China produces 35% of the world's coal mine output, but accounts for 80% of the global death toll caused by coal mining; most mine accidents are caused by illegal underground mining (Hindu 2009). Therefore, it is necessary to monitor illegal mining activities in mining areas efficiently and accurately.

Interferometric synthetic aperture radar (InSAR) technology has been widely used in the monitoring of surface subsidence in mining areas owing to its advantages of low cost, all-weather, all-day, and high-

precision operation (Wang et al. 2017; Chuang et al. 2021; Fan et al. 2021; Yuan et al. 2021). Ground subsidence occurs after underground coal mining, and the characteristics of surface deformation are shown in a series of concentric circles or concentric ellipses on the InSAR interferogram, which are called "mining subsidence basins" (Wang et al. 2021). Therefore, scholars can monitor illegal mining by detecting mining subsidence basins on the InSAR interferogram. However, with the continuous development of InSAR technology, the image amplitude is also increasing. Visual search alone has an extensive artificial error and consumes considerable energy to search for mining subsidence basins in a wide range of interferograms. Therefore, it is necessary to determine a method to find mining subsidence basins in the InSAR interferogram automatically. In recent years, the development of computer hardware and large-scale data collection has helped convolutional neural networks (CNNs) to achieve excellent computer vision results, such as image classification and image detection (Ren et al. 2016). Alzubaidi et al. (Alzubaidi et al. 2022) presented a machine learning-based approach for automatic fracture recognition from unwrapped drill-core images. Zhang et al. (Zhang et al. 2022) proposed a mask labelling methodology that can establish a large and diverse training set without manual labelling. Xinhong et al. (Shi et al. 2021) proposed a method based on the Domain adaptive Faster RCNN called adaptive threshold cascade Faster RCNN. Liu Fang et al. (Fang et al. 2021) applied a deep learning algorithm to the automatic detection and recognition of Oracle bone rubbings to facilitate the research and popularization of traditional culture. CNNs have been widely applied in various industries, but have not been applied to mining subsidence basin detection by scholars. Therefore, in this study, we introduce the CNN method for mining subsidence basin detection using a large-width InSAR interferogram.

To effectively monitor illegal mining in large areas and prevent geological disasters, the CNN model, which has achieved excellent results in image detection, is applied to the detection of mining subsidence basins in the InSAR interferogram. By introducing AlexNet, VGG19, and ResNet50 CNN models and using the support vector machine (SVM) model with strong classification ability to replace the original Softmax classifier of the CNN model, the CNN_SVM automatic detection method of mining subsidence basin is constructed, The improved ResNet50_AFSA_SVM mining subsidence basin monitoring model is constructed by introducing artificial fish swarm algorithm. This method can effectively detect mining subsidence basins in a large-width InSAR interferogram. In addition, it provides a scientific basis for monitoring mining activities and preventing geological disasters, and offers essential reference significance for landslides and other geological disasters.

Methodology

CNN model principle

A typical CNN model comprises a convolution layer, pooling layer, full connection layer, and softmax classification function. A CNN has a vital feature of adaptive extraction, and its mechanism of parameter sharing and inter-layer connection sparsity introduced within the hidden layer can significantly reduce the number of model parameters. Three classical CNNs are adopted in this study, and their principles are as follows.

AlexNet uses an eight-layer neural network with five convolutional layers, three fully connected layers, and a maximum pooling layer. The entire deep learning network contains 630 million links, 60 million parameters, and 650 000 neuron nodes (Zhao et al. 2021). The AlexNet structural model is shown in Figure 1.

The main difference between AlexNet architecture and traditional CNNs is the increase in network depth, which leads to an increase in the number of tunable parameters of the model and regularization techniques, such as random inactivation and data enhancement. Random deactivation techniques are applied after the first two fully connected layers in the AlexNet architecture, resulting in less overfitting and better generalization to unknown examples. Another remarkable feature of AlexNet is the use of ReLU nonlinear activation after each convolutional and fully connected layer, which significantly improves the training efficiency compared to the traditionally used hyperbolic tangent function.

VGGNet explores the relationship between the depth of a CNN and its performance, and by iteratively stacking small convolutional kernels of 3 × 3 and maximum pooling layers of 2 × 2; VGGNet successfully constructs a CNN with 16 to 19 layers of depth (Blok et al. 2021). The network structure is shown in Figure 2.

VGGNet has five convolutional segments with two to three convolutional layers in each segment, and a maximum pooling layer is connected at the end of each segment to reduce the image size. The same number of convolutional kernels are contained within each segment, with more convolutional kernels in the later segments: 64-128-256-512-512. Multiple identical 3 × 3 convolutional layers are often stacked together, which is a functional design.

The ResNet50 network structure comprises several residual modules. Assuming that is the input data and with $F(x)$ denoting the residual mapping, the characteristic output $H(x)$ of the network residual module is

$$H(x) = F(x) + x$$

1

When $F(x) = 0$, it means that the convolutional layer performs constant mapping; when $F(x) > 0$, it means that the convolutional layer learns new feature information, ensuring gradient transfer during backpropagation, which effectively solves the problem of gradient disappearance and network degradation during network training (Nijat et al. 2019). The ResNet50 network structure is illustrated in Figure 3.

The ResNet50 network structure comprises 49 convolutional layers and one fully connected layer, and the network operation process comprises six phases. The first stage contains convolution, batch regularization, activation function, and maximum pooling operations; the CONV (CONVOLUTION) BLOCK in the second to fifth stages represents the convolution residual block, the ID (IDENTITY) BLOCK

represents the constant residual block, and the sixth stage contains the global average pooling, fully connected layer, and softmax classifier.

AFSA algorithm principle

Artificial fish swarm algorithm was first proposed by Li Xiaolei et al in the study of optimizing mode of animal autonomous body(Li et al. 2004), AFSA's rationale is that artificial fish as a whole can be described as $Z = \{X_1, X_2, X_3 \cdots, X_i, \cdots, X_M\}$, *M* is the total number of *AF*, $X_i = (x_1, x_2, \cdots, x_n)$ represents the individual state of *AF*, x_i is the variable to be optimized, The food concentration of the current position of the artificial fish is $Y = f(X)$, Where is the target function value, The distance between artificial fish individuals is denoted as $d = \left|X_i - X_j\right|$, $Visual$ represents the perceived distance of the artificial fish, $Step$ is the maximum stride length of the artificial fish, δ is the crowding factor, 0 < δ < 1.

(1) Foraging behavior. The current state of the artificial fish is X_i. In its perception range, randomly select a state as X_j, $X_j = X_i + rand(\cdot) \times Visual$, and $rand(\cdot)$ represents any random number between 0 and 1. Compare the food concentration function twice. When $Y_i < Y_j$, move one step in this direction; On the contrary, select a state X_j for comparison. After repeatedly trying the maximum number of times, if the advance conditions of the artificial fish are still not met, move forward one step at random. The formula is

$$X_{inext} = \begin{cases} X_i + rand(\cdot) \cdot Step \cdot \dfrac{x_j - x_i}{\left|x_j - x_i\right|} & Y_i < Y_j \\ X_i + rand(\cdot) \cdot Step & Y_i > Y_j \end{cases} \quad (2)$$

(2) Clustering behavior. The number n_0 of artificial fish in the current field of vision, the position X_c of artificial fish in the cluster center, and the food concentration Y_c of artificial fish in the center. When $\frac{Y_c}{n_0} > \delta Y_i$, move one step in this direction, otherwise, conduct foraging behavior,

$$X_{inext} = \begin{cases} X_i + rand(\cdot) \cdot Step \cdot \dfrac{X_c - X_i}{\left|X_c - X_i\right|} & \dfrac{Y_c}{n_0} > \delta Y_i \\ \text{Foraging behavior} & \dfrac{Y_c}{n_0} < \delta Y_i \end{cases} .(3)$$

(3) Rear end behavior. X_j is the artificial fish with the smallest Y_j in the current field of vision. When $\frac{Y_j}{n_0} > \delta Y_i$, move one step in this direction, otherwise, foraging behavior will be carried out,

$$X_{inext} = \begin{cases} X_i + rand(\cdot) \cdot Step \cdot \dfrac{X_j - X_i}{\left| X_j - X_i \right|} & \dfrac{Y_j}{n_0} > \delta Y_i \\ \text{Foraging behavior} & \dfrac{Y_j}{n_0} < \delta Y_i \end{cases} \quad (4)$$

Firstly, the artificial fish is randomly generated in the parameter interval, the food concentration function (objective function) is calculated, and the optimal value is recorded. Secondly, the state of each artificial fish after the above three behaviors is compared with the optimal value. If it is better than the optimal value, it will be replaced. After gen (total number of iterations) iterations, the state of artificial fish is the optimal state.

The quality of SVM algorithm depends on the value of penalty factor *c* and kernel function parameter *g*(Qin et al. 2021). in this paper, the artificial fish swarm algorithm with strong optimization ability and good global convergence is used to find the optimal penalty factor *c* and kernel function parameter *g*, The Resnet50_AFSA_SVM mining subsidence basin detection model is constructed(Mrozek and Perlicki 2019; Khan et al. 2021).

Method construction

To effectively monitor illegal mining in large areas and prevent geological disasters, the CNN model, which has achieved excellent results in image detection, is applied to the detection of mining subsidence basins in InSAR interferograms. By introducing the CNN model and using the SVM model with a strong classification ability to replace the original Softmax classifier of the CNN model, in this study, we constructed a CNN_SVM automatic detection method for mining subsidence basins. The application process of this method is as follows:

(1) Constructing sample datasets: Interferograms were obtained by processing Sentinel-1A radar data using differential radar interferometry (D-InSAR), manually cropping the mined subsidence basin as a positive sample dataset, and selecting other targets as a negative sample dataset.

(2) CNN extracts feature vectors: The CNN model is used to extract the features of the mining subsidence basin and other targets, and the extracted feature vectors are input into the SVM classifier.

(3) SVM classifier: After the feature vector was introduced into the SVM classifier, the artificial fish swarm algorithm searched for the optimal penalty factor *c* and the kernel function parameter *g*, and used the SVM classifier for training and classification test to test the model accuracy.

(4) Detection of mining subsidence basin: After model is trained and tested, it starts to find mining subsidence basins found in the large-width InSAR interferogram, which uses non-maximal value suppression to remove the duplicate search box, and finally outputs the mining subsidence basin detection results. The flow of the method is shown in Figure 4.

Evaluation criteria

In this study, the precision rate *P*, recall rate *R*, and *F*1 value are chosen to evaluate the accuracy of the method detection, which is formulated as follows:

$$\begin{cases} P = \dfrac{TP}{TP + FP} \\ R = \dfrac{TP}{TP + FN} \\ F1 = \dfrac{2PR}{P + R} \end{cases}$$

5

Among them, the meaning of each indicator is shown in Table 1.

Table 1
Meaning of each index.

	Positive forecast	Negative forecast
Actual positive	TP	FN
Actual negative	FP	TN

The precision rate represents the proportion of samples classified as positive cases that are actually positive, and the recall rate represents the proportion of detected positive samples to the total number of actual positive samples; the value of F1 reflects the comprehensive identification ability of positive and negative samples, and the higher the value of F1, the more robust the method (El-Saadawy et al. 2021).

Experiments And Results

Study area

To verify the method used in this study, the Huainan mining area with many subsidence basins and apparent subsidence was adopted as the test area. The Huainan mining area is located in the north central part of Anhui Province, with a geographical range of approximately 116 ° 21 21 " E–117 ° 11 59 "E and 32 ° 32 45 " N–33 ° 00 24 "N, as shown in Figure 5. The Huainan mining area is bounded by the Huaihe River, the Panxie new mining area in the north, and the old mining area in the south. The continuous large-scale mining of the Huainan coalfield has not only made important contributions to the national economic construction, but has also caused significant ecological and environmental problems (Chen et al. 2016).

Built datasets

Seven "sentinel-1A" IW mode images of Huainan mining area from November 16, 2017, to January 27, 2018, were downloaded in this study, and six interference images were generated through DInSAR data processing. The detailed image parameters are listed in Table 2.

Table 2
Sentinel-1A interference pairs used to construct training samples.

Serial number	Main image	Auxiliary image	Path number	Time baseline(D)	Spatial baseline(M)
1	2017-11-16	2017-11-28	142	12	22.2
2	2017-11-28	2017-12-10	142	12	31.7
3	2017-12-10	2017-12-22	142	12	-44.9
4	2017-12-22	2018-01-03	142	12	-28.6
5	2018-01-03	2018-01-15	142	12	-31.7
6	2018-01-15	2018-01-27	142	12	-50.8

From the interferograms formed by the six interference pairs shown in Table 2, the mining subsidence basin targets and other non-mining subsidence basin targets were selected as the sample datasets. A total of 120 mining subsidence basins were considered as the positive sample datasets, and 180 non-mining subsidence basins were considered as the negative sample datasets. Some sample datasets are shown in Figure 6.

Results and analysis

In this study, we used 80% of the selected datasets as the training dataset and 20% as the validation dataset. AlexNet, VGG19, and ResNet50 were used for image feature extraction, and the SVM classifier was used to classify and evaluate the accuracy of the extracted feature vectors. The precision rate *P*, recall rate *R*, and *F*1 value were selected to evaluate the accuracy of the method detection. The accuracies of the three CNN_SVM models are listed in Table 3.

Table 3
CNN_SVM model accuracy table.

CNN models	P	R	F1
AlexNet_SVM	0.927	0.927	0.927
VGG19_SVM	0.929	0.951	0.940
ResNet50_SVM	0.952	0.976	0.964
ResNet50_AFSA_SVM	0.976	0.976	0.976

From Table 3, we can observe that the accuracy of the above three models combined with the SVM model for mining subsidence basin detection is higher than 90%, and the accuracy of ResNet50_AFSA_SVM model constructed in this paper is up to 97.6%. After the models were trained and tested, large-formatted wide InSAR interferograms were used for mining subsidence basin detection using the trained models. In this study, interferometric pairs comprising 2-view "Sentinel-1A" IW mode images from November 28, 2018, to December 10, 2018, were selected for detection, and the results are shown in Table 4. The accuracy rate refers to the ratio of the number of mining subsidence basins detected by the model to the number of all mining subsidence basins in the interferogram, and the miss detection rate refers to the ratio of the number of undetected mining subsidence basins to the number of all mining subsidence basins in the interferogram.

Table 4
Test results.

CNN models	Number to be tested (pc)	Number of correct detections (pc)	Accuracy rate (%)	Missing detection rate (%)
AlexNet_SVM	43	33	76.7%	23.3%
VGG19_SVM	43	34	79.1%	20.9%
ResNet50_SVM	43	36	83.7%	16.3%
ResNet50_AFSA_SVM	43	38	88.3%	11.7%

The CNN_SVM automatic detection method of the mining subsidence basin constructed in this study is applied to mining subsidence basin detection on the InSAR interferogram of the Huainan Mining area. The method can detect most mining subsidence basins, The ResNet50_AFSA_SVM model has the highest accuracy of 88.3%. The detection results are shown in Figure 7. In this study, it was found that a small number of undetected mining subsidence basins are mining areas with tiny subsidence areas or are areas with inferior interference quality. The CNN_SVM model constructed in this study is not effective in detecting when the edge features of mining subsidence basins are not obvious. Scholars further discussed and analyzed this method to improve the detection effect and scalability of the proposed method.

Discussions

(1) Impact of increasing the datasets on the method

To discuss the influence of the number of datasets on the CNN_SVM automatic detection method for mining subsidence basins owing to the limited number of interference maps of the mining subsidence basin, the data set of the mining subsidence basin map is expanded by translation and rotation. With 180 mining subsidence basins as positive sample datasets and 240 non-mining subsidence basins as negative sample datasets, the experimental results of the ResNet50_AFSA_SVM model are shown in Table 5.

Table 5
ResNet50_AFSA_SVM model expanded dataset detection results.

Datasets	Number to be tested (pc)	Number of correct detections (pc)	Accuracy rate (%)	Missing detection rate (%)
Original datasets	43	38	88.3%	11.7%
Adding datasets	43	39	90.6%	9.4%

The accuracy of the ResNet50_AFSA_SVM model for detecting mining subsidence basins was 90.6% after expanding datasets, which was higher than 88.3%. It can be observed that the expanded datasets improved the accuracy of model detection, but the detection effect was still poor for some areas with no apparent characteristics of mining subsidence basins.

(2) Effect of changing the proportion of the datasets on the method

This study used 80% of the selected datasets as the training dataset and 20% as the validation dataset. To explore whether the change in the ratio of the training datasets and Validation datasets is the effect of the CNN_SVM method to detect the mining subsidence basin, in this study, we conducted two experiments for the ResNet50_AFSA_SVM model with +10% of the training datasets and -10% of the Validation datasets and -10% of the training datasets and +10% of the Validation datasets, and the results of the experiments are shown in Table 6.

Table 6
ResNet50_AFSA_SVM model changes the detection result of datasets proportion.

Dataset proportion	Number to be tested (pc)	Number of correct detections (pc)	Accuracy rate (%)	Missing detection rate (%)
Original datasets	43	38	88.3%	11.7%
Training datasets+10% Validation datasets-10%	43	39	90.6%	9.4%
Training datasets-10% Validation datasets+10%	43	36	83.7%	16.3%

It can be observed from Table 6 that changing the proportion of datasets has a slight influence on the accuracy of the ResNet50_AFSA_SVM model in detecting mining subsidence basins, and the detection effect of mining subsidence basins with obscure image features is still poor.

(3) Scalability study of the method

The method used in this study was successfully applied to the Huainan mining area. Wu et al. (Wu et al. 2021) proposed the early identification and monitoring of landslides based on InSAR technology and optical remote sensing. Next, scholars will apply the method proposed in this study to detect the surface deformation characteristics caused by landslides and other geological disasters to monitor and prevent landslides and other geological disasters.

Conclusions

(1) A CNN_SVM automatic detection method of mining subsidence basins is constructed in this study and can be applied to the detection of mining subsidence basins with large-width InSAR interferograms. The method provides a scientific basis for the government to monitor illegal mining activities and prevent geological disasters in mining areas. In the next step, scholars will apply this method to detect surface deformation features caused by other geological hazards, such as landslides, which will help monitor and prevent geological hazards.

(2) The method was applied to the Huainan mine area. The experimental results show that the three models detect mining subsidence basins with an accuracy of approximately 80%, and ResNet50_SVM detects mining subsidence basins with an accuracy of 86.0%, which is better than AlexNet_SVM and VGG19_SVM. The accuracy of the improved Resnet50_SVM based on AFSA algorithm is 88.3%, which is better than the unimproved Resnet50_SVM model. Through further discussion and analysis of the method, the accuracy of Resnet50_AFSA_SVM for mining subsidence basin detection is improved by adding datasets.

(3) A small number of mining subsidence basins with inconspicuous edge features are poorly detected by the CNN_SVM mining subsidence automatic detection method constructed in this study. The authors will

consider increasing the datasets and using higher-resolution InSAR data to enhance the detection effect.

Declarations

Author Contributions

Conceptualization, L.W. and S.L.; methodology, L.W.; software,S.L.; validation, C.J., C.T. and J.L.; formal analysis, Z.L.; investigation, J.H.; resources, S.L.; data curation, S.L.; writing—original draft preparation, S.L.; writing—review and editing, L.W.; visualization, L.W.; supervision, L.W.; project administration, L.W. All authors have read and agreed to the published version of the manuscript.

Funding

This research was funded by the National Natural Science Foundation of China under Grant Nos.52074010, 41602357, by the Anhui Science Fund for Distinguished Young Scholars(No. 2108085Y20), and by the Graduate innovation fund project of Anhui University of Science and Technology (No. 2021cx2142).

Institutional Review Board Statement

Not applicable.

Informed Consent Statement

Not applicable.

Data Availability Statement

Not applicable.

Acknowledgments

The authors are grateful to the editor and anonymous reviewers for their valuable suggestions which greatly help to improve the original manuscript.

Conflicts of Interest

The authors declare no conflict of interest.

References

1. Alzubaidi F, Makuluni P, Clark SR, Lie JE, Mostaghimi P, Armstrong RT (2021) Automatic fracture detection and characterization from unwrapped drill-core images using mask R–CNN. J Pet Sci Eng 208:109471

2. Blok PM, van Evert FK, Tielen APM, van Henten EJ, Kootstra G (2021) The effect of data augmentation and network simplification on the image-based detection of broccoli heads with Mask R-CNN. J Field Robot 38(1):85–104
3. Chen Y, Yuan L, Chong XU (2016) Investigation on using mining subsidence area to build a reservoir in Huainan Coal Mining Area. J China Coal Soc 41(11):2830–2835
4. Chuang J, Lei W, Xue-Xiang Y, Shenshen C, Tao W, Zhongchen G (2021) A DPIM-InSAR method for monitoring mining subsidence based on deformation information of the working face after mining has ended. Int J Remote Sens 42(16):6330–6358
5. El-Saadawy H, Tantawi M, Shedeed HA, Tolba MF (2021) A hybrid two-stage CNN-SVM model for bone X-Rays classification and abnormality detection. Int J Sociotechnology Knowl Dev 13(4):50–65
6. Fan H, Wang L, Wen B, Du S (2021) A new model for three-dimensional Deformation extraction with single-track InSAR based on mining subsidence characteristics. Int J Appl Earth Obs Geoinf 94:102223
7. Fang L, Huabiao L, Jin M, Sheng Y, Peiran J (2021) Research of Automatic Detection and Recognition of Oracle Rubbings Based on Mask-RCNN. 1-12
8. Hindu T (2009), July 14 "Illegal mining: Lokayukta slams government." Retrieved November 25, 2021, from http://www.hindu.com/2009/07/14/stories/2009071461270100.htm
9. Khan MA, Akram T, Zhang Y-D, Sharif M (2021) Attributes based skin lesion detection and recognition: A mask RCNN and transfer learning-based deep learning framework. Pattern Recogn Lett 143:58–66
10. Li X, Xue YC, Fei L (2004) Parameter estimation method based on artificial fish swarm algorithm. Journal of Shandong University (Engineering Edition) 3:84–87
11. Mrozek T, Perlicki KT (2019) Simultaneous monitoring of the phenomena of CD, Crosstalk, and OSNR in the physical layer of the optical network with the use of convolutional neural networks. Opt Quantum Electron 53(11):1–16
12. Nijat K, Shi Q, Liu S, Bilal I, Li H (2019) Automatic classification method of oasis plant community in desert hinterland based on VGGNet and ResNet models. Trans Chin Soc Agric Mach 50(1):217–225
13. Qin J, Zhang Y, Zhou H, Yu F, Sun B, Wang Q (2021) Protein crystal instance segmentation based on mask R-CNN. Crystals 11(2):157
14. Ren S, He K, Girshick R, Sun J (2016) Faster R-CNN: towards real-time object detection with region proposal networks. IEEE Trans Pattern Anal Mach Intell 39(6):1137–1149
15. Shi X, Li Z, Yu H (2021) Adaptive threshold cascade faster RCNN for domain adaptive object detection.Multimed Tools Appl:1–18
16. Wang L, Zhang XN, Chen YF (2017) Method of mining subsidence prediction parameters inversion based on D-Insar LOS deformation. J China Univ Min Technol 46(05):1159–1165
17. Wang Z, Li L, Wang J, Liu J (2021) A method of detecting the subsidence basin from InSAR interferogram in mining area based on HOG features. J China Univ Mini Technol 50(02):404–410

18. Wu L, Wang J, Fu Y (2021) Early identifying and monitoring landslides in Guizhou province with InSAR and optical remote sensing. Surv Mapp Bulletin 7:98–102
19. Yuan M, Li M, Liu H, Lv P, Li B, Zheng W (2021) Subsidence monitoring Base on SBAS-InSAR and slope stability analysis method for damage analysis in mountainous mining subsidence regions. Remote Sens 13(16):3107
20. Zhang Z, Yin X, Yan Z (2022) Rapid data annotation for sand-like granular instance segmentation using mask-RCNN. Autom Constr 133:103994
21. Zhao X, Dong C, Zhou P, Zhu M, Ren J, Chen X (2021) Research on wind turbine blade damage diagnosis based on UAV machine vision. Acta Energ Sol Sin 42(07):390–397
22. Zhu J, Li Z, Hu J (2017) Research progress and methods of InSAR for deformation monitoring. Acta Geod Cartogr Sin 46(10):1717–1733

Figures

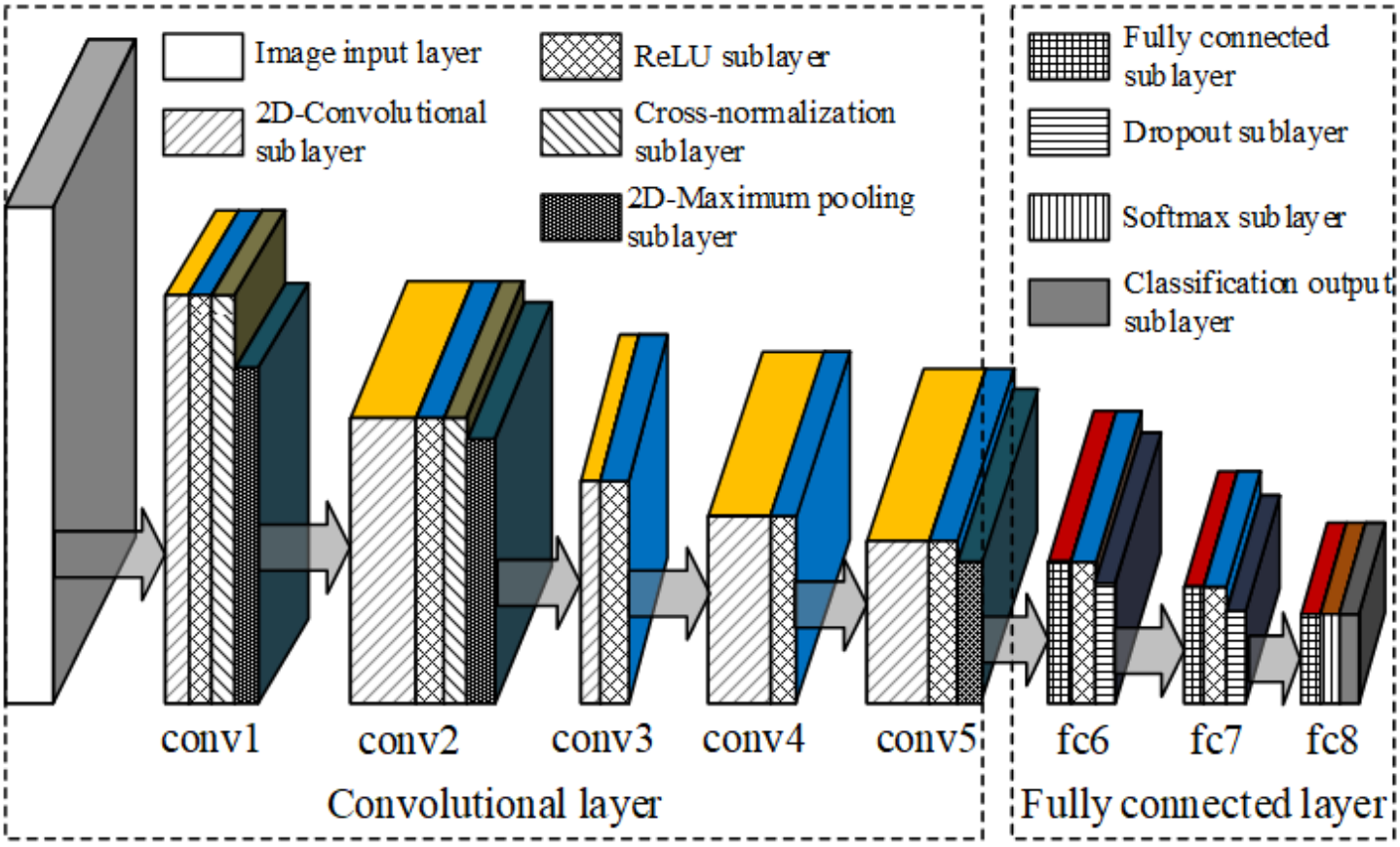

Figure 1

Schematic of AlexNet network structure.

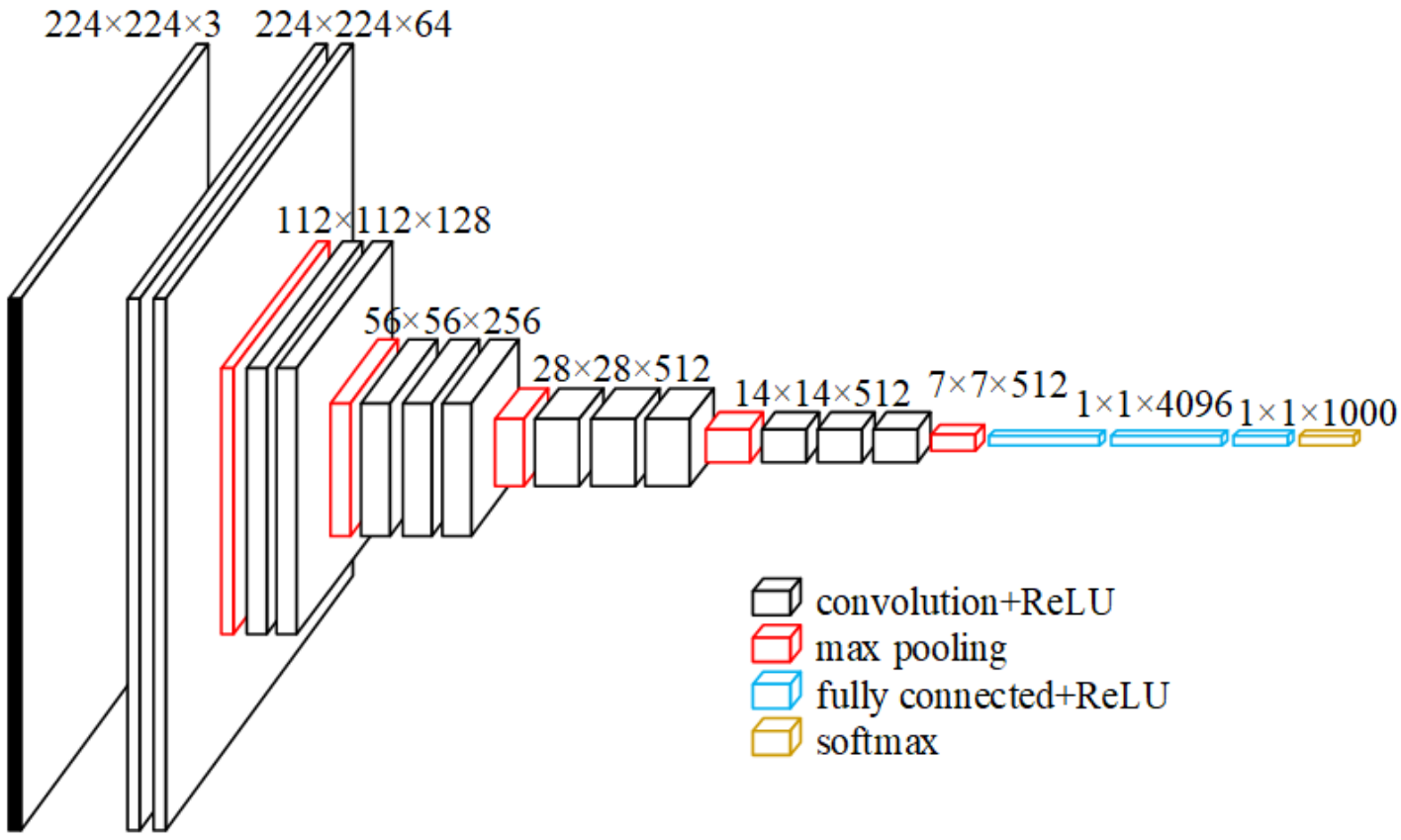

Figure 2

Schematic of VGG19 network structure.

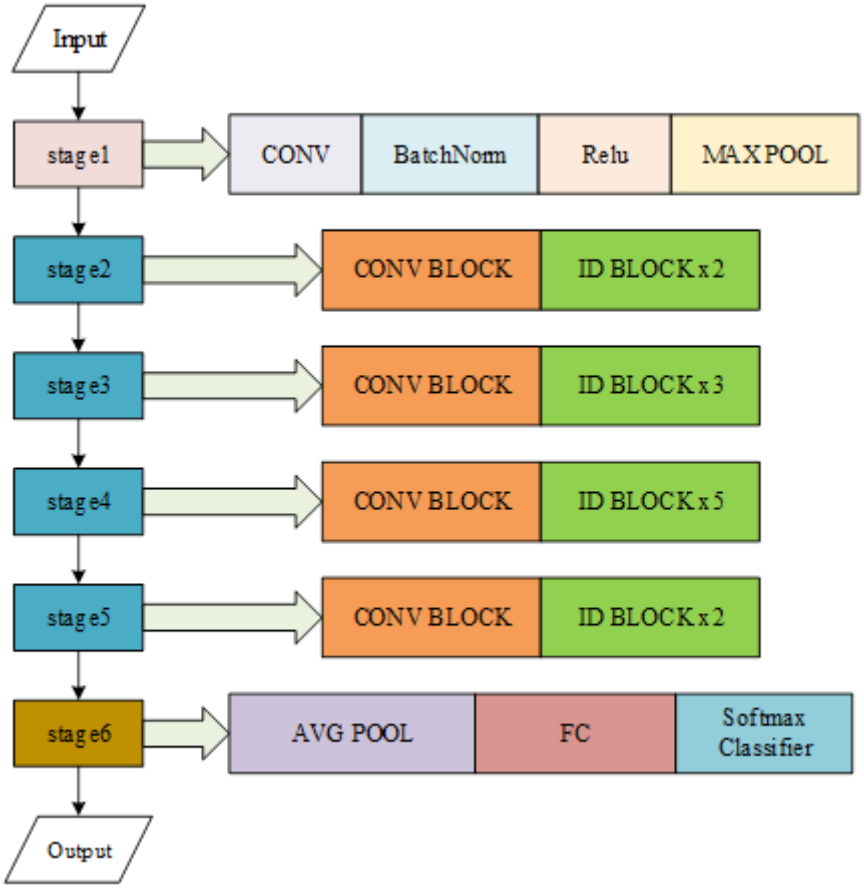

Figure 3

ResNet50 network structure diagram.

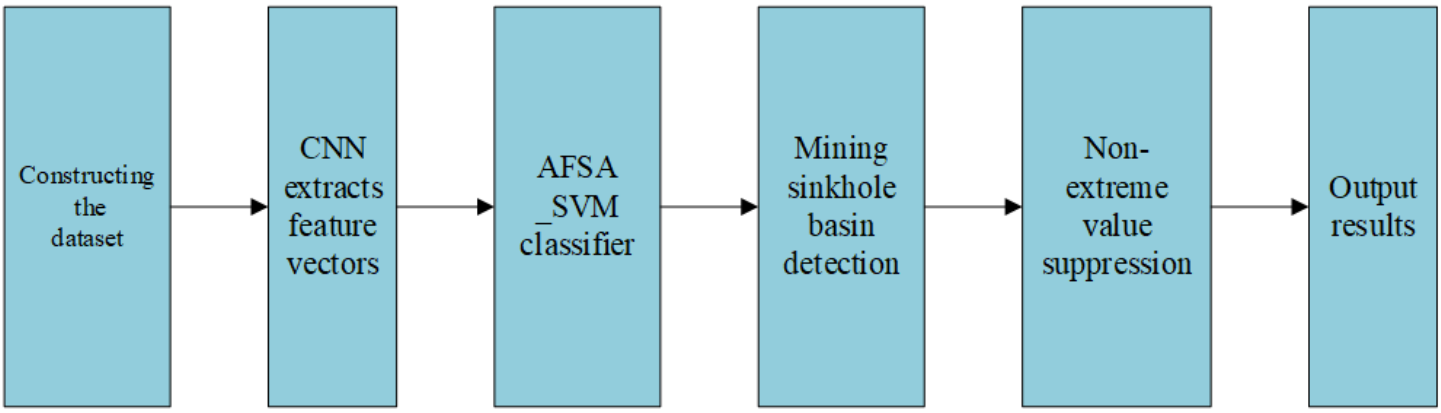

Figure 4

Method overall flow chart.

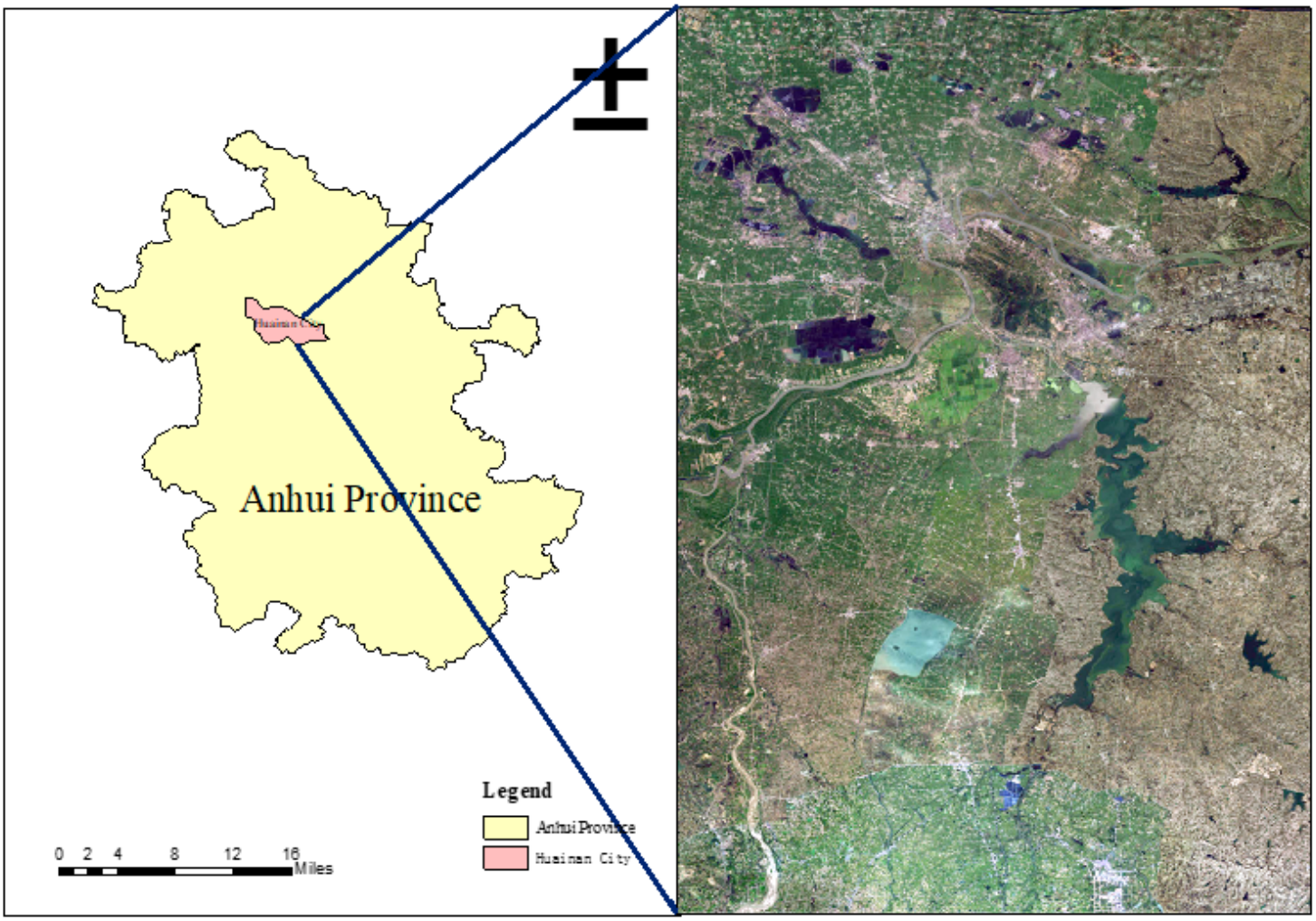

Figure 5

Geographical location of Huainan Mining Area.

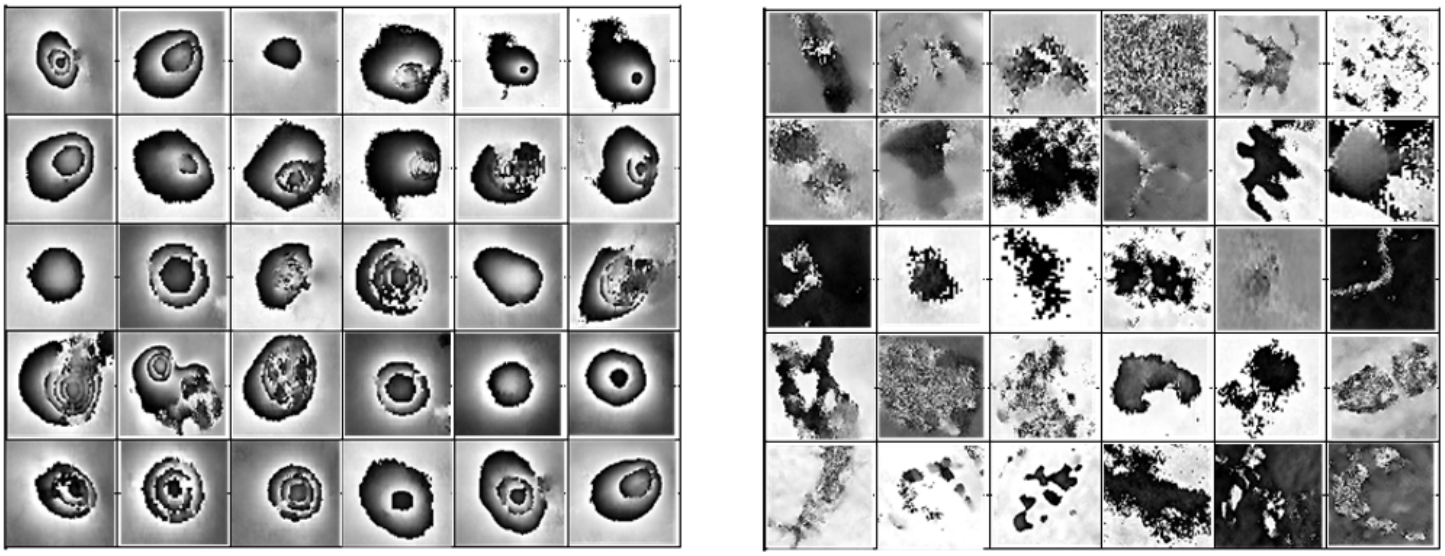

Figure 6

Sample datasets (partial).

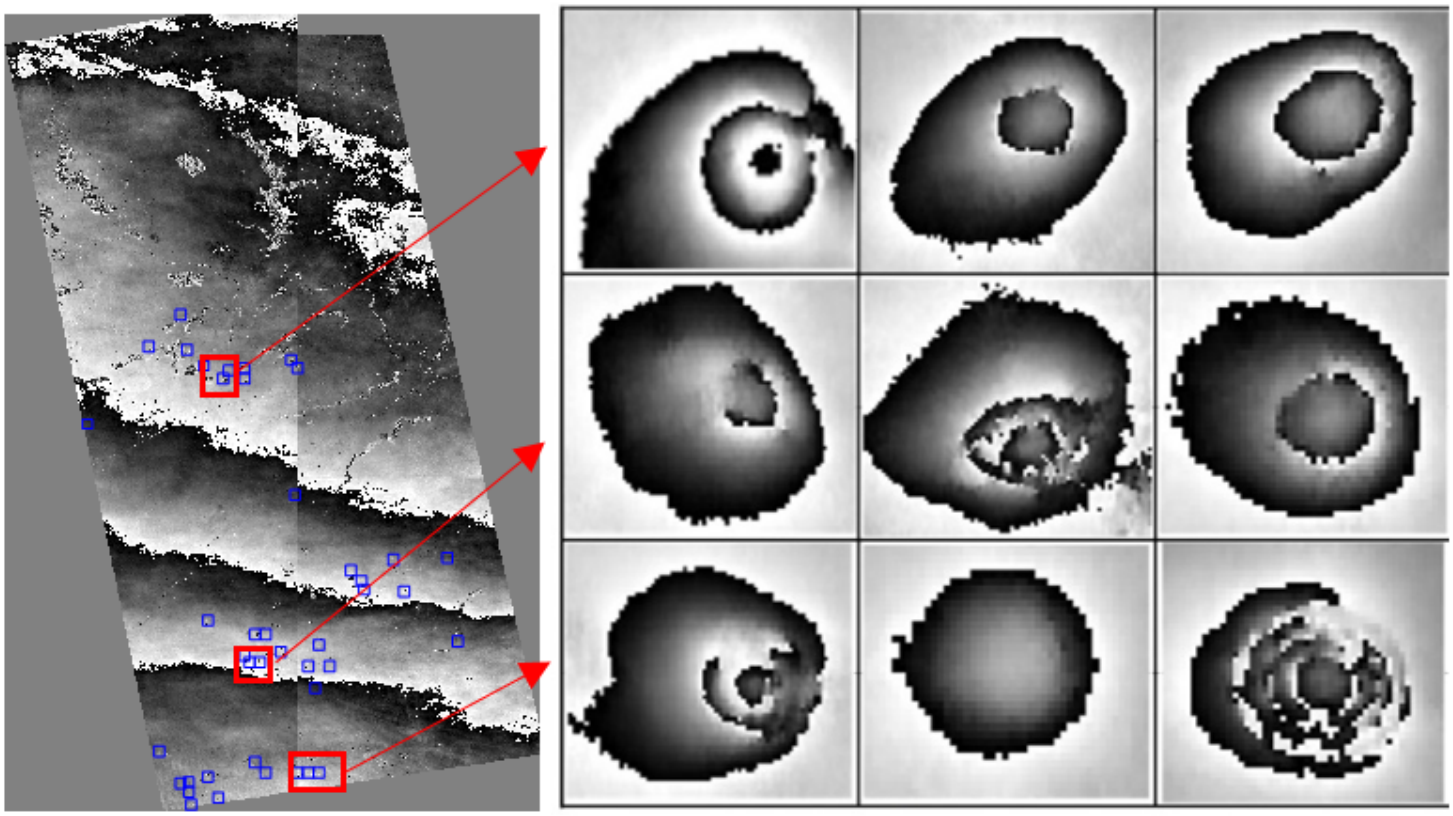

Figure 7

ResNet50_AFSA_SVM model detection result diagram.